Nanoscale Advances

ROYAL SOCIETY OF CHEMISTRY

PAPER

View Article Online
View Journal | View Issue

Check for updates

Cite this: *Nanoscale Adv.*, 2025, **7**, 3028

Efficient photoelectrochemical oxidation of benzyl alcohol in a microchannel flow cell using compact and mesoporous TiO_2 photoanodes

Sirachat Sattayarak and Paravee Vas-Umnuay *

Photoelectrochemical (PEC) conversion presents a viable strategy for reducing the external bias required in conventional electrochemical methods for organic molecule valorization. However, the efficiency of PEC processes is largely dependent on photoelectrode characteristics, specifically light absorption and charge transport properties. These properties are crucial for efficient generation of charge carriers and photocurrent for driving reactions. Herein, we report efficient PEC conversion of benzyl alcohol to benzaldehyde using tailored TiO_2 photoanodes of both compact and mesoporous film morphologies in a continuous-flow PEC cell. Notably, our PEC flow cell was designed on a microscale to facilitate superior mass transfer. Parameters such as applied potential, electrolyte flow rate, channel width, and photoanode characteristics were systematically investigated to elucidate their impact on conversion efficiency and selectivity in the PEC oxidation process. The results indicated that at an applied potential of 3.5 V and an electrolyte flow rate of 0.05 ml min^{-1}, the microchannel with a width of 0.1 mm, which corresponds to a residence time of 1.6 min, achieved benzyl alcohol conversion exceeding 80%. Comparative analyses with traditional batch H-cells revealed over a fivefold increase in benzyl alcohol conversion in the microchannel flow cell with the mesoporous TiO_2 photoanode. Additionally, the flow cell exhibited approximately threefold higher benzaldehyde selectivity compared to batch reactors employing the compact TiO_2 photoanode. Overall, this work demonstrates the potential of continuous-flow microchannels with tailored photoanodes for achieving efficient and rapid PEC conversions, promising advancements in sustainable organic transformations.

Received 11th December 2024
Accepted 23rd March 2025

DOI: 10.1039/d4na01032a

rsc.li/nanoscale-advances

Open Access Article. Published on 24 March 2025. Downloaded on 2/22/2026 7:25:42 PM.
This article is licensed under a Creative Commons Attribution-NonCommercial 3.0 Unported Licence.

1 Introduction

The increasing global energy demand, depletion of non-renewable resources, and worsening climate change resulting from fossil fuel consumption have prompted efforts to develop sustainable and environmentally friendly energy storage and conversion technologies. Biomass and biomass-derived compounds emerge as uniquely renewable and abundant sources of carbon for the production of fuels and value-added chemicals. In addition, integrating renewable energy sources, such as solar energy, for the solar-driven conversion of biomass-derived chemicals to valuable products represents a critical research area in advancing sustainable economies. Among various approaches, photoelectrochemical (PEC) processes are extensively employed to drive redox reactions by harnessing light energy. While considerable research has focused on PEC water splitting to generate hydrogen, other potentially valuable chemical products have been relatively underexplored.[1] Although PEC water splitting offers notable advantages, the hydrogen evolution reaction (HER) at the cathode is a non-spontaneous process requiring a minimum voltage of 1.23 V.[2–4] Moreover, the oxygen evolution reaction (OER) at the anode is the rate-limiting step due to its slower reaction kinetics compared to the HER.[5] Notably, the sluggish OER can be replaced by more favorable oxidation reactions involving organic compounds, *e.g.*, biomass-derived alcohols and their derivatives, which typically have an oxidation potential lower than 1.23 V.[2,5,6] Recent advancements suggest that PEC technology can be effectively employed to convert these organic compounds into valuable chemicals, thus presenting a promising avenue for advancing the green economy.

Among various organic molecules, benzyl alcohol is of particular interest due to its potential derivation from biomass feedstocks and therefore can be treated as a typical lignin model compound.[7] Furthermore, benzyl alcohol undergoes oxidative cleavage to yield benzaldehyde, a valuable chemical intermediate widely used in the fragrance, flavoring, and pharmaceutical industries.[8–10] Benzaldehyde is currently produced primarily through chemical methods that involve the use of toxic reagents and generate harmful byproducts.[2,6] PEC oxidation, on the other hand, offers a more environmentally friendly route by utilizing solar energy as the driving force, with the potential to integrate

Center of Excellence in Particle and Material Processing Technology, Department of Chemical Engineering, Faculty of Engineering, Chulalongkorn University, Bangkok 10330, Thailand. E-mail: Paravee.V@chula.ac.th

© 2025 The Author(s). Published by the Royal Society of Chemistry

Open Access Article. Published on 24 March 2025. Downloaded on 2/22/2026 7:25:42 PM. This article is licensed under a Creative Commons Attribution-NonCommercial 3.0 Unported Licence.

renewable energy sources into chemical manufacturing. In this process, benzyl alcohol is adsorbed onto the surface of a semiconductor electrode which is used as a photoelectrode, and upon illumination, electron–hole pairs are generated within the semiconductor, driving the oxidation reaction on the electrode surface. This method offers several advantages over conventional thermal or catalytic oxidation processes, including reduced energy consumption, minimized byproducts, and enhanced selectivity.[11]

The efficiency and selectivity of PEC oxidation depend on several factors, including the choice of the photoelectrode material, electrode structure, operating conditions, and reactor design. By optimizing these parameters, it is possible to achieve high yields of benzaldehyde while minimizing the formation of side products. Among photoelectrode materials, titanium dioxide (TiO_2) has emerged as a prominent choice for photoanodes due to its chemical stability, non-toxicity, and ability to generate photocurrent under UV light irradiation.[10,12] It was first utilized as the photoanode in photocatalytic water splitting in a photoelectrochemical (PEC) cell studied by Fujishima and Honda in the early 1970s[13] and has since become a key reference in subsequent research. In addition to TiO_2, bismuth vanadate ($BiVO_4$) has later become a widely used photoanode in PEC reactions,[14,15] owing to its ability to absorb visible light and thus utilize a broader portion of the solar spectrum. While $BiVO_4$ demonstrates good photocatalytic activity, its efficiency is often hindered by sluggish interfacial reaction kinetics. To overcome this limitation, research has increasingly focused on composite materials, such as the deposition of a V_2O_5 layer on $BiVO_4$ to enhance the surface activity of the photoanode.[7] Additionally, Luo *et al.* employed a Co-based layered double hydroxide (LDH) combined with graphene to enhance $BiVO_4$.[14] The excellent electrical conductivity of graphene facilitated the transfer of photogenerated electrons from the conduction band (CB) of LDH to the CB of $BiVO_4$, while photogenerated holes moved from $BiVO_4$ to LDH due to the more negative valence band (VB) level of LDH. This configuration effectively reduced the recombination of photogenerated carriers and promoted the oxidation of benzyl alcohol. Furthermore, tungsten trioxide (WO_3) is well-known for its stability and photocatalytic activity under ultraviolet (UV) light, although its effectiveness is constrained by its limited light absorption range.[16] Despite the various materials used as photoanodes, TiO_2 remains one of the most commonly employed options for PEC applications due to its stability in most chemical environments, ease of synthesis, and relatively low cost compared to other materials. These advantages are crucial for practical applications and scalability. However, its performance is often limited by poor charge carrier mobility and a limited surface area available for reaction.[17] To address these challenges, recent advancements have focused on optimizing TiO_2 photoanodes through structural modifications. In particular, the development of mesoporous TiO_2 structures has shown significant promise in enhancing photoelectrochemical performance by increasing surface area and improving charge carrier transport.

The design of the PEC reactor is another crucial factor in optimizing the performance of the PEC oxidation process.[18–20] An effective reactor design should facilitate efficient light absorption and mass transfer of reactants and products. To date, most previous research has utilized a simple H-type cell for PEC applications,[21] where the cathode and anode compartments are separated by an ion-exchange membrane. Despite the simplicity of the system setup, the reaction time is relatively long, typically exceeding 4 h.[7,22–29] Recent advancements have introduced a continuous flow microchannel as a more effective alternative. These reactors offer several advantages, including improved mixing and enhanced mass and heat transfer due to laminar flow conditions.[30–33] The continuous flow setup ensures a more uniform exposure of the photoanode to the reactants and light, thereby accelerating the reaction and reducing the time required to achieve high yields. Additionally, the high surface-to-volume ratio in flow reactors enhances the interaction between light and the photoanode material, further improving the efficiency of the oxidation process. To the best of our knowledge, no experimental implementation of PEC oxidation of benzyl alcohol to benzaldehyde using a microchannel flow cell has been reported elsewhere, except for our simulation study. Our previous simulation results indicated that the electrolyte flow velocity and the width of electrolyte channels were the key factors influencing product formation. The optimized design and operating parameters achieved a maximum conversion of benzyl alcohol of 48.25% with 100% selectivity for benzaldehyde.[34] However, further modifications to these parameters could potentially enhance the efficiency of the PEC oxidation process.

In this work, a basic flat plate design of the PEC microchannel flow cell was constructed and employed to facilitate the oxidation of benzyl alcohol within the anode channel. We demonstrated that the continuous flow cell was highly effective for PEC oxidation. Furthermore, we systematically optimized key parameters, including applied potential, electrolyte flow rate, and channel width of the flow cell to achieve the highest conversion efficiency and selectivity in the PEC oxidation process. Although there has been considerable research on the PEC oxidation of benzyl alcohol to benzaldehyde using TiO_2-based photoanodes in batch systems, this study is, to our knowledge, the first to compare the performance of different TiO_2 photoanode morphologies, compact *vs.* mesoporous films, in a continuous-flow PEC system.

2 Experimental

2.1 Materials

Ethyl alcohol (C_2H_5OH, >99.9%) and hydrochloric acid (HCl, 37%) were purchased from Quality Reagent Chemical. Pluronic P123 and benzyl alcohol ($C_6H_5CH_2OH$, >99%) were purchased from Sigma Aldrich. Titanium(IV) isopropoxide (Ti$[OCH(CH_3)_2]_4$, TTIP, >98%) was purchased from Thermo Scientific. Isopropyl alcohol (C_3H_7OH) was purchased from CARLO ERBA Reagents. Sodium sulfate (Na_2SO_4, 98%) was purchased from LOBA CHEMIE. These chemicals were used without any further treatment or purification.

2.2 Preparation and characterization of compact and mesoporous TiO_2 thin films

2.2.1 Substrate preparation. Fluorine-doped tin oxide (FTO) glasses (4 cm × 8 cm), used as the substrate for

Open Access Article. Published on 24 March 2025. Downloaded on 2/22/2026 7:25:42 PM. This article is licensed under a Creative Commons Attribution-NonCommercial 3.0 Unported Licence.

photoanodes, were cleaned with a commercial detergent solution followed by rinsing with deionized (DI) water. Then, clean substrates were subsequently sonicated with DI water and isopropanol for 15 min each, respectively. Finally, they were dried in flowing nitrogen and treated with UV-ozone for 15 min.

2.2.2 Preparation of precursor solution for compact and mesoporous TiO_2 thin films. To prepare compact TiO_2 films, 785 μl of 0.35 M TTIP and 18 μ of 0.04 M HCl were dissolved in 5 ml of ethanol separately and stirred with a magnetic stirrer at 400 rpm under ambient conditions for 15 min. Then, the HCl solution was injected into the TTIP solution drop by drop with continuous stirring at the same speed for 15 min until the solution became transparent.

On the other hand, to prepare mesoporous TiO_2 films, 1.34 ml of 2.88 M HCl solution was added into 2.56 ml of 0.55 M TTIP solution with continuous stirring under ambient conditions. To prepare a surfactant solution, 0.35 g of Pluronic P123 was added into 11.40 ml of ethanol and stirred until the solution was completely dissolved. Finally, the surfactant solution was added into the TTIP solution and continuously stirred for another 30 min.

2.2.3 Film deposition and characterization. Compact and mesoporous TiO_2 thin films were deposited on FTO glasses by the rapid convective deposition (RCD) method. RCD has been widely used to fabricate thin films from a colloidal solution as a result of evaporation flow and/or viscous drag force when the solution is dragged using a blade across the substrate.[35] This technique offers several advantages over other solution-based deposition methods, *e.g.*, efficient utilization of a very small amount of precursor solution, thereby generating very low waste of materials. To deposit compact and mesoporous TiO_2 films, the precursor solutions prepared from Section 2.2.3 were injected between the tip of the blade and the substrate surface. The solution was being pulled in the opposite direction and coated on the substrate surface when the substrate was moved at a constant speed of 500 μm s^{-1}. A thin layer of precursor solution was fully covered on the substrate and then heated on a hot plate at 70 °C for 15 min. The procedure was repeated 3 times to obtain the desired thickness of TiO_2 films. Finally, the deposited compact films were annealed in a N_2 atmosphere at 500 °C for 1 h to crystallize the TiO_2 structure, whereas the deposited mesoporous films were annealed at 450 °C in order to prevent collapse of the porous structure.

The surface and cross-sectional morphologies of compact and mesoporous TiO_2 thin films were analyzed by field emission scanning electron microscopy (FESEM; Hitachi, SU8230). The phase formation was examined using X-ray diffraction (XRD; Bruker AXS Model D8 Discover equipped with a Cu Kα source). The optical properties were determined using a UV-vis spectrophotometer (Shimadzu UV-2600) within a wavelength range of 250–800 nm. The optical bandgap (E_g) of TiO_2 films was estimated from the Tauc plot, where the intercept of the linear portion of the plot of $(\alpha h\nu)^2$ against $(h\nu)$ on the $(h\nu)$ axis gives the bandgap. The specific surface area and the pore size distribution of the sample of TiO_2 powder from compact and mesoporous films were measured using the Brunauer–Emmett–Teller (BET) method using a BELSORP-MINI II system. High performance liquid chromatography (HPLC) equipped with a C18 column was used to analyze liquid products from the reactor.

2.3 Microchannel PEC flow cell description

The design of a PEC flow cell for benzyl alcohol oxidation was based on our previous work, where the reactor was designed in a flat plate configuration with a continuous flow of electrolyte solution and benzyl alcohol using computational fluid dynamics (CFD) simulation. Fig. 1(a) illustrates the components of the fabricated PEC flow cell, consisting of frames, where one side has a hole to allow supplying solar incident light, rubber gaskets, a copper plate as the cathode, TiO_2/FTO as the light-responsive photoanode, Teflon sheets with 0.1 mm thickness as microchambers for reactions, aluminum foil, and a Nafion® 117 proton exchange membrane, separating two chambers. The flow cell was constructed with a height of 120 mm and a width of 80 mm. The photoelectrode height was 40 mm and width was 20 mm, subjected to a solar irradiation area of 800 mm^2. The volumes of both chambers were 1 ml. A syringe pump was used to supply the electrolyte and precursor solutions into the chambers continuously.

2.4 Photoelectrochemical benzaldehyde production

The reaction was carried out under ambient conditions. Both catholyte and anolyte solutions of 0.1 M Na_2SO_4 were continuously fed into the chambers at flow rates ranging from 0.05–0.20 ml min^{-1} using syringe pumps separately. 0.02 M benzyl alcohol was mixed and introduced with the anolyte solution

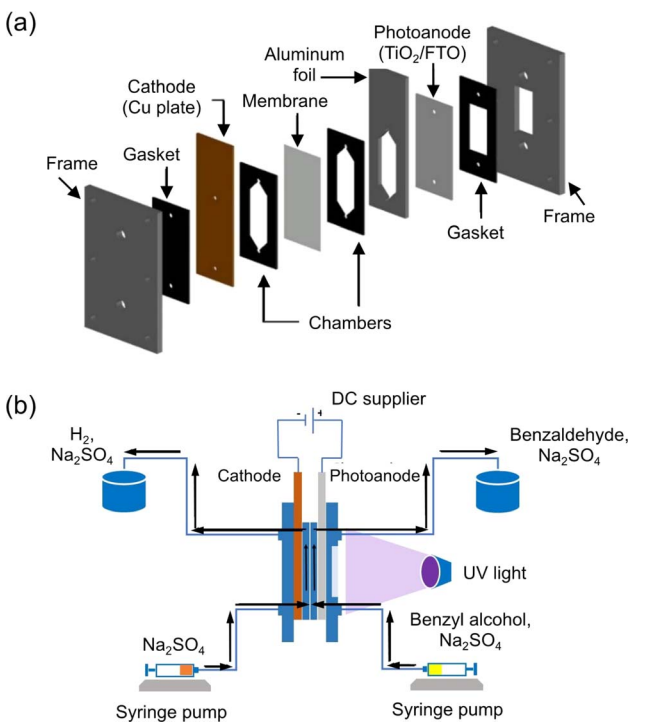

Fig. 1 Schematic diagram of the (a) components of the microchannel PEC flow cell and (b) experimental setup.

© 2025 The Author(s). Published by the Royal Society of Chemistry

Open Access Article. Published on 24 March 2025. Downloaded on 2/22/2026 7:25:42 PM. This article is licensed under a Creative Commons Attribution-NonCommercial 3.0 Unported Licence.

into the anodic compartment. The PEC flow cell was connected to a DC power supply with a copper wire to control the applied potential for the reaction. The PEC oxidation of benzyl alcohol was evaluated under 100 W of UV illumination on the photoanode (equivalent to 20 mW cm^{-2}), where liquid samples were collected and measured at the outlet of the reactor every 15 min. A detailed description of the experimental setup can be seen in Fig. 1(b). The concentration of products obtained in each experiment was calculated. The experiment under each condition was repeated three times to calculate the average conversion of benzyl alcohol and selectivity of benzaldehyde.

3 Results and discussion

3.1 Characterization of compact and mesoporous TiO_2 photoanodes

In the present study, two different morphologies of compact and mesoporous TiO_2 thin films with approximately similar thickness were prepared to compare various aspects of properties as photoanodes for PEC oxidation of benzyl alcohol. Fig. 2(a) shows the top morphology of the compact TiO_2 film on the FTO substrate. The uniform and crack-free film, with particle size ranging from 30–50 nm, was achieved. As seen in the cross-sectional view of the film in Fig. 2(b), the film thickness was ~310 ± 10 nm. The surface was smooth and densely packed. On the other hand, the mesoporous TiO_2 film was obtained from the introduction of structure-directing agent Pluronic P123 into the precursor solution, as shown in Fig. 2(c). A rough surface was formed compared to that of the compact film. A slightly fluffy layer was also observed in the side view of the film, as shown in Fig. 2(d). The film thickness was controlled to be approximately the same as that of the compact

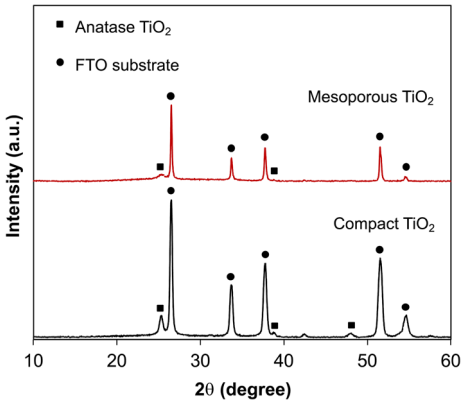

Fig. 3 XRD patterns of compact and mesoporous TiO_2 films deposited on FTO substrates.

TiO_2 film by adjusting concentrations of TTIP and HCl. The obtained thickness was ~320 ± 15 nm. By eliminating the film thickness factor between both films, different morphologies resulting in different surface areas and optical and electrical properties are major factors to evaluate the performance of PEC oxidation of benzyl alcohol.

The crystallinity of TiO_2 films was characterized using XRD, as shown in Fig. 3. The crystalline structure of both compact and mesoporous TiO_2 films was detected with the peaks of 2θ at 25.29°, 38.70° and 47.97° referring to the planes (101), (004), and (200), respectively, which demonstrated the anatase phase of TiO_2 films. It should be noted that the intensity of diffraction peaks of the mesoporous film is smaller due to lower calcination temperature.

To compare the specific surface area of different morphologies of TiO_2 films, both compact and mesoporous TiO_2 film

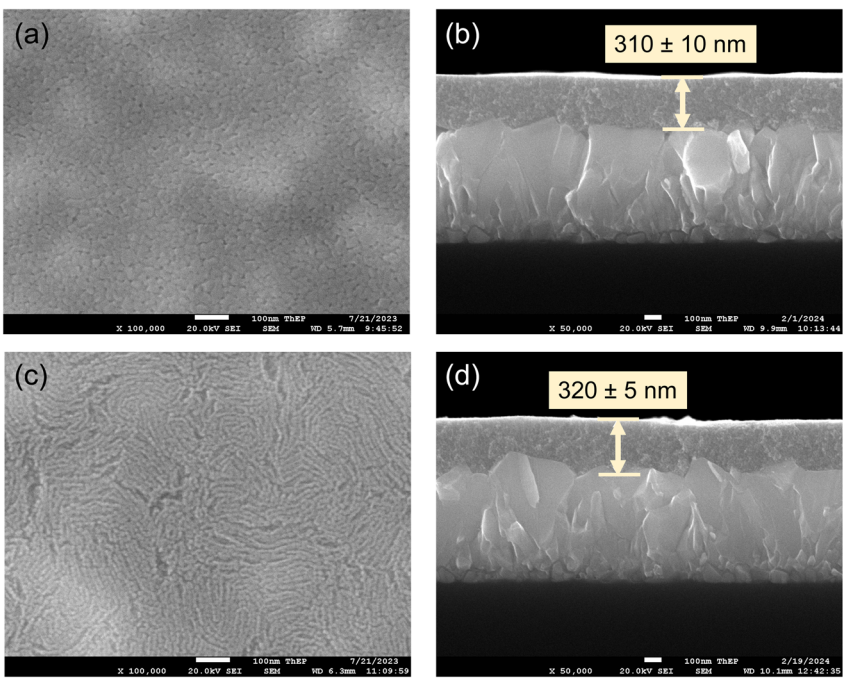

Fig. 2 Surface FESEM of (a) compact and (c) mesoporous TiO_2 films, and cross-sectional images of (b) compact and (d) mesoporous TiO_2 films.

Open Access Article. Published on 24 March 2025. Downloaded on 2/22/2026 7:25:42 PM.
This article is licensed under a Creative Commons Attribution-NonCommercial 3.0 Unported Licence.

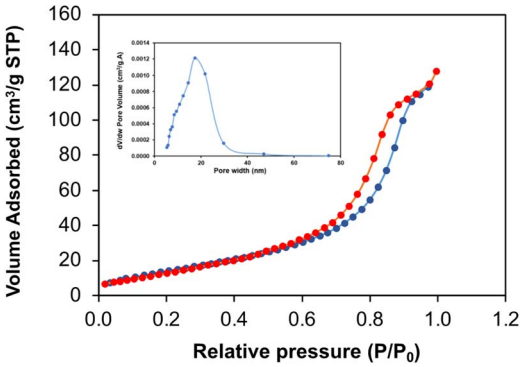

Fig. 4 Nitrogen adsorption/desorption isotherm of the mesoporous TiO_2 film. The inset shows the pore size distribution of the mesoporous TiO_2 film.

samples were scratched off from the substrate for BET analysis. It was found that the surface areas obtained from the compact and mesoporous TiO_2 films were 9.65 and 57.41 $m^2\ g^{-1}$, respectively, confirming that the porous structure is beneficial for the increase of specific surface area of about 6 fold. In addition, the result was supported by the nitrogen adsorption/desorption isotherm of the mesoporous TiO_2 film presented in Fig. 4. The sample exhibited a mesoporous structure and displayed a typical type IV isotherm, revealing the shape of the hysteresis loop. The pore volumes of samples were in the range of 0.197–0.198 $cm^3\ g^{-1}$, while the average pore diameters were in the range of 17.42–17.43 nm, as shown in the inset of Fig. 4. A large surface area, pore volume and pore diameter of the mesoporous TiO_2 film were expected to enhance reaction–diffusion behavior for improving photoelectrochemical oxidation of benzyl alcohol.

Fig. 5(a and b) show the absorption spectra of the compact and mesoporous TiO_2 films, respectively, exhibiting strong absorption of ultraviolet (UV) light. Therefore, the photoelectrochemical oxidation of benzyl alcohol using both compact and mesoporous TiO_2 films can be carried out using UV light. The optical bandgaps obtained from both TiO_2 films were determined to be approximately 3.76 eV, as shown in the insets of Fig. 5.

3.2 PEC oxidation of benzyl alcohol using the microchannel flow cell

The photoelectrochemical results obtained using the compact TiO_2 film as the photoanode are present in Fig. 6. The experiments were performed at a flow rate of 0.1 ml min^{-1} in the continuous-flow microchannel under three different conditions: in the dark, under natural light, and under UV illumination. The experiments were conducted with an applied voltage of 3.5 V and without any applied voltage. The conversion (C) of benzyl alcohol and selectivity (S) of benzaldehyde were determined as follows:

$$C(\%) = \frac{[BA]_0 - [BA]_0}{[BA]_0} \times 100\% \quad (1)$$

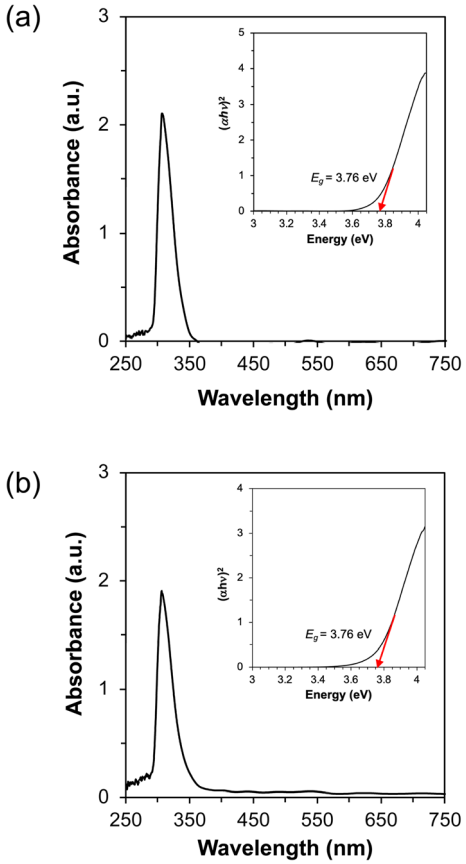

Fig. 5 Optical absorption spectra of (a) compact and (b) mesoporous TiO_2 films. The insets show estimated band gaps from the optical absorption spectra of both films.

$$S(\%) = \frac{[BD]}{[BA]_0 - [BA]} \times 100\% \quad (2)$$

where $[BA]_0$ is the initial concentration of benzyl alcohol and [BA] and [BD] are the concentrations of benzyl alcohol and benzaldehyde, respectively, at a given time during the photoelectrochemical reaction. As expected, the highest conversion of benzyl alcohol of about 60% carried out under the presence of UV illumination was achieved, while those carried out under natural light and dark conditions achieved a conversion of about 40% and 35%, respectively. Similarly, the selectivity of benzaldehyde obtained under the presence of UV illumination was also the highest at about 30%. In addition, without applied voltage between the photoanode and cathode under UV light, very low conversion of benzyl alcohol and selectivity of benzaldehyde were obtained. Therefore, these preliminary investigations indicated that the reaction requires both UV illumination and applied voltage for oxidation of benzyl alcohol into benzaldehyde.

According to previous investigation, applied potential is one of the critical parameters in the reaction process. It must be carefully controlled to avoid detrimental effects such as electrode degradation or inefficient energy use. Therefore, determining the optimal applied potential is essential to enhance the

© 2025 The Author(s). Published by the Royal Society of Chemistry

Open Access Article. Published on 24 March 2025. Downloaded on 2/22/2026 7:25:42 PM. This article is licensed under a Creative Commons Attribution-NonCommercial 3.0 Unported Licence.

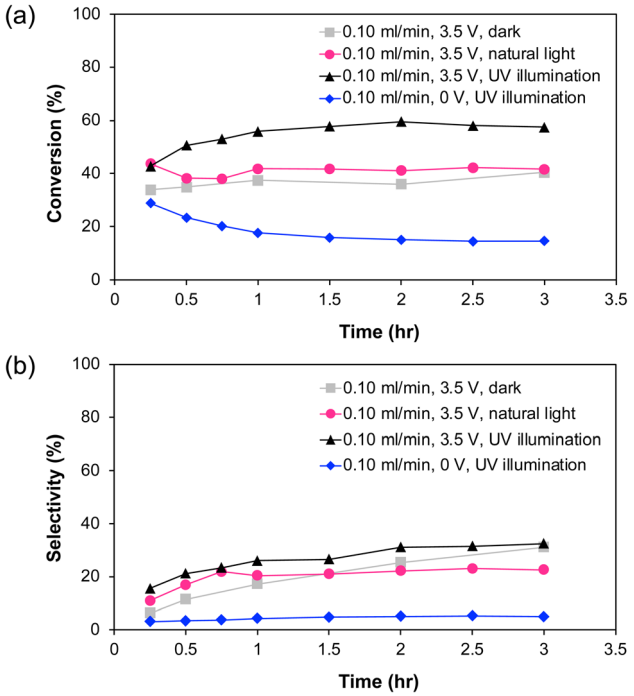

Fig. 6 (a) Conversion of benzyl alcohol and (b) selectivity of benzaldehyde obtained in the dark, in the presence of natural light and under UV illumination, and without applied voltage conditions, at a flow rate of 0.10 ml min^{-1} using the compact TiO_2 film as the photoanode.

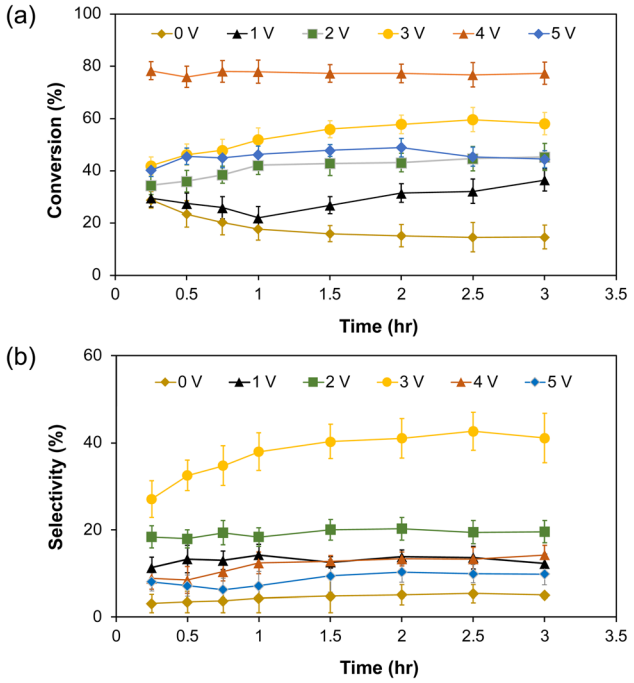

Fig. 7 (a) Conversion of benzyl alcohol and (b) selectivity of benzaldehyde obtained at a flow rate of 0.10 ml min^{-1} using the compact TiO_2 film as the photoanode at different applied potentials.

PEC system's efficiency. In this study, the applied potential was varied from 0–5 V for the reaction operated with a flow rate of 0.1 ml min^{-1} using the compact TiO_2 film as the photoanode. As shown in Fig. 7(a), an enhancement in benzyl alcohol conversion was observed with increasing applied potential. Higher potential can increase the number of charge carriers generated on the photoanode surface and provide more driving force for the separation of photogenerated charges. In addition, the rate of electron transfer can be accelerated, thereby enhancing the oxidation rate and subsequent benzyl alcohol conversion. However, declining conversion was observed beyond a maximum peak of 4 V. This was attributed to the consequence of the excessive potential that resulted in degradation of the TiO_2 film (image not shown). In terms of the selectivity of benzaldehyde, increasing the applied potential can have several effects on the PEC reaction. As shown in Fig. 7(b), the selectivity of the reaction towards benzaldehyde reached a maximum at an applied potential of 3 V and then decreased at 4 V and 5 V, respectively. In our work, increasing the potential favored the reaction pathway towards the desired product over another. On the other hand, applying excessively high potential could lead to side reactions or generation of unwanted reactive species which can decrease the selectivity of the process. Moreover, at 5 V, this decline was attributed not only to the side reactions but also to the degradation of TiO_2, as observed in the actual film, where most of it detached from the substrate after the reaction. Thus, the following experiments were based on an applied potential of 3.5 V, where its conversion is slightly higher than that at 3 V and its selectivity is higher than that at 4 V.

In addition to the operating conditions, a physical dimension represented using the channel width of the PEC flow cell can significantly influence the performance of the reaction. The channel width is a factor responsible for holding electrolyte and facilitating mass transport. In this investigation, the channel width through which the electrolyte solutions and reactant flowed was varied to 0.1, 0.2, and 0.3 mm, while maintaining a constant flow velocity of 0.05 ml min^{-1} and a residence time of 0.8 min. This variation in channel width corresponded to flow rates of 0.1 ml min^{-1}, 0.2 ml min^{-1}, and 0.3 ml min^{-1}, respectively. Fig. 8(a) depicts an increase in conversion of benzyl alcohol with decreasing channel width. A similar trend was also observed for the selectivity, as shown in Fig. 8(b). This can be explained by that a narrower channel typically enhances mass transport due to a reduced diffusion distance and a higher surface area-to-volume ratio, which leads to better mixing and more efficient reactions. This allows the fresh reactant to reach the electrode surface more quickly and products to be swept away, improving reaction kinetics and conversion rate. Likewise, the reduced diffusion distance between the bulk reactants and the electrode surface in narrower channels also improves the interaction between the reactants and TiO_2, promoting the desired product and minimizing the chances of side reactions. Nonetheless, the conversion and selectivity achieved from the PEC flow cell with 0.1 mm channel width were limited at about 58% and 30%, respectively, due to the fixed residence time. The effects of the electrolyte flow rate with varying residence times were therefore studied in the following study.

The compact and mesoporous TiO_2 films that were previously prepared as photoanodes were used in the following study

© 2025 The Author(s). Published by the Royal Society of Chemistry

Open Access Article. Published on 24 March 2025. Downloaded on 2/22/2026 7:25:42 PM.
This article is licensed under a Creative Commons Attribution-NonCommercial 3.0 Unported Licence.

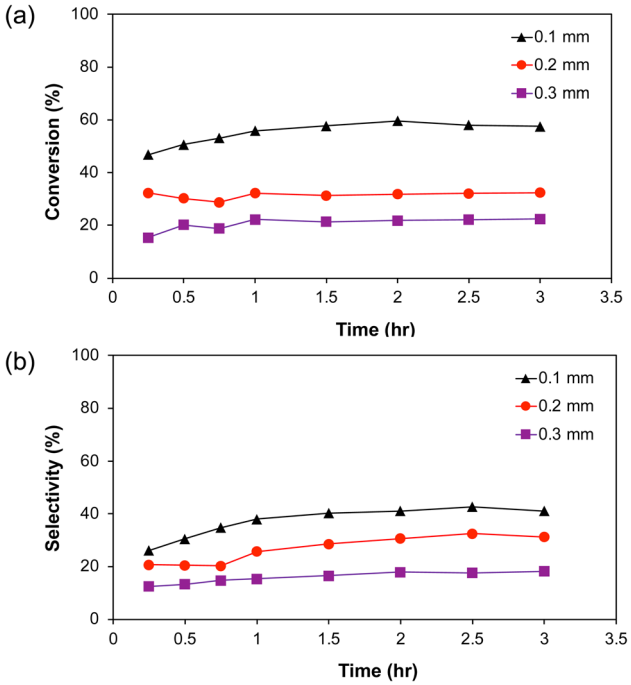

Fig. 8 (a) Conversion of benzyl alcohol and (b) selectivity of benzaldehyde obtained at a fixed flow rate of 0.10 ml min^{-1} using the compact TiO_2 film as the photoanode in the PEC flow cell with different channel widths.

to investigate the effects of the electrolyte flow rate for comparison. The flow rates ranging from 0.05–0.20 ml min^{-1} were applied in the PEC flow cell with a channel width of 0.1 mm and an applied potential of 3.5 V. The electrolyte flow rate determines how long the reactants stay in contact with the electrode surface. Lower flow rates offer a certain duration for the surface reaction, therefore achieving higher conversion of benzyl alcohol. Fig. 9(a and b) reveal that the highest conversions of approximately 82% and 85% were achieved with the lowest controlled flow rate of 0.05 ml min^{-1}, which corresponds to a residence time of 1.6 min, for compact and mesoporous TiO_2 films, respectively. Interestingly, Fig. 9(c and d) reveal a contrasting trend where the highest selectivity, reaching approximately 62% and 52%, was achieved from the highest flow rate for compact and mesoporous TiO_2 films, respectively. This can be explained in terms of different physical properties of compact and mesoporous TiO_2 films used as photoanodes in the system that led to variations in conversion and selectivity obtained at different flow rates. The mesoporous film distinctively offers high surface area which provides more sites for reactant adsorption on the photoanode surface, as well as light absorption, potentially resulting in higher overall conversion compared to the compact film. However, the porous structure can also act as a pathway for charge recombination, which may reduce conversion efficiency. In terms of selectivity, the denser structure of the compact film helped suppress unwanted side reactions occurring on the photoanode surface, thereby improving selectivity, while high surface area of the mesoporous structure provided more sites for unwanted reactions, potentially impacting selectivity of benzaldehyde. It can be observed that the difference in conversion and selectivity between these two films is not as large as expected, mainly due to the influence of various factors such as flow rates and other

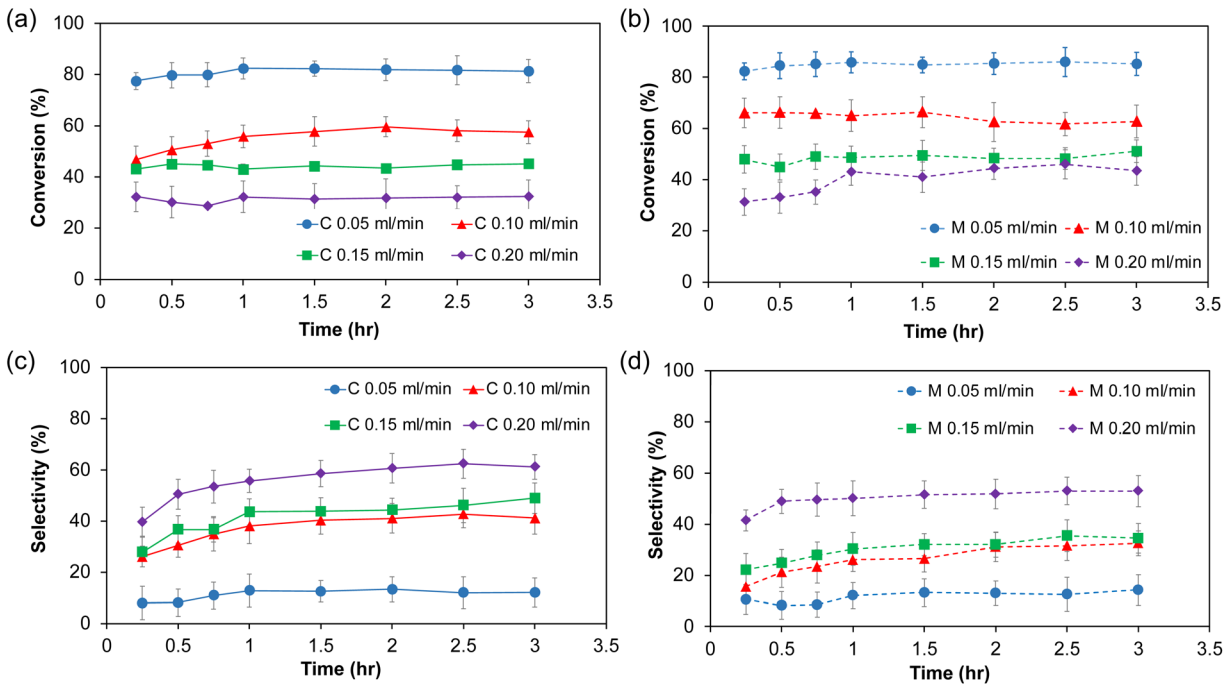

Fig. 9 Conversion of benzyl alcohol obtained from the reaction using (a) compact TiO_2 film and (b) mesoporous TiO_2 film, and selectivity of benzaldehyde obtained from the reaction using (c) compact TiO_2 film and (d) mesoporous TiO_2 film as photoanodes with various electrolyte flow rates.

© 2025 The Author(s). Published by the Royal Society of Chemistry

Open Access Article. Published on 24 March 2025. Downloaded on 2/22/2026 7:25:42 PM. This article is licensed under a Creative Commons Attribution-NonCommercial 3.0 Unported Licence.

experimental conditions. However, the physical properties of the films, such as surface area and porosity, play a significant role in the overall performance. As a result, the reaction outcome is influenced by the combined effect of all these parameters, leading to the observed differences in conversion and selectivity.

A significant advantage of the microchannel operated in a continuous flow regime lies in the ability to maintain a constant reactant concentration throughout the reaction. This is achieved by continuously introducing fresh reactants through the microchannel, while simultaneously removing products. In contrast, batch reactors experience a progressive decrease in the reactant concentration as the reaction proceeds due to lack of continuous replenishment. We performed PEC experiments using a batch H-cell to facilitate comparison with the continuous-flow microchannel system. Flow rates of 0.05 ml min^{-1} and 0.2 ml min^{-1} were investigated, where the highest conversion and selectivity were achieved, respectively. As shown in Fig. 10(a), the conversion of benzyl alcohol slowly increases, reaching only 16% after a 6-h reaction time, whereas the conversion of benzyl alcohol obtained from the microchannel using both compact and mesoporous TiO_2 photoanodes exceeded 80% within the first 30 min after the reaction started, demonstrating an over fivefold increase compared to the batch reactor conditions. Similarly, the selectivity of benzaldehyde exhibits a gradual increase obtained from the batch H-cell, reaching only approximately 22% after 6 h of reaction time, as illustrated in Fig. 10(b). According to the comparative study, it clearly demonstrates that the continuous flow regime and the microscale design of the PEC cell developed in this study significantly enhanced mass transfer and reaction kinetics, leading to notable improvements in both conversion and selectivity.

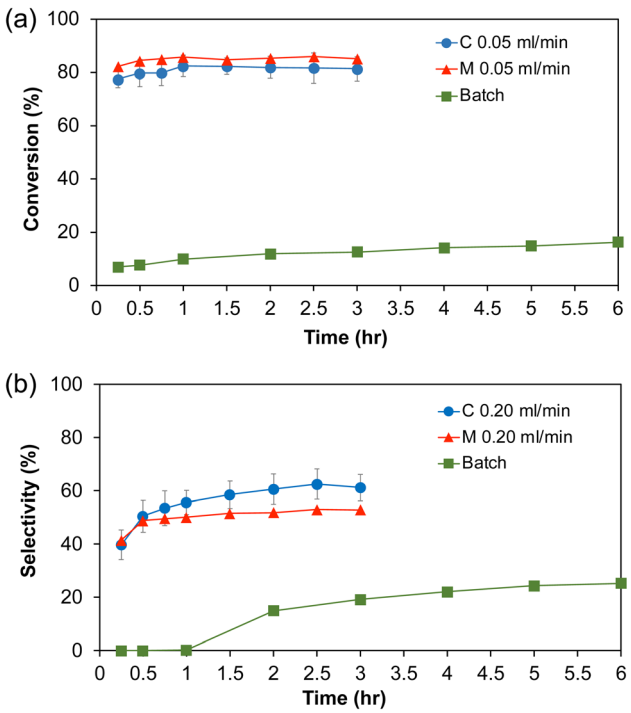

Fig. 10 (a) Highest conversion of benzyl alcohol and (b) highest selectivity of benzaldehyde using the compact TiO_2 film and mesoporous TiO_2 film as photoanodes obtained from the PEC flow cell compared with that of the batch setup.

4 Conclusions

This study successfully demonstrated the efficient PEC conversion of benzyl alcohol to benzaldehyde using a continuous-flow microchannel flow cell by applying compact and mesoporous TiO_2 films as photoanodes. Operating parameters included an applied potential of 3.5 V and an electrolyte flow rate of 0.05 ml min^{-1} in the fabricated PEC flow cell with a channel width of 0.1 mm, resulting in benzyl alcohol conversion exceeding 80%. The microscale design facilitated superior mass transfer, leading to significantly enhanced reaction kinetics compared to traditional batch H-cells. Notably, the PEC microchannel flow cell achieved over a fivefold increase in benzyl alcohol conversion compared to the batch reactor using the mesoporous TiO_2 photoanode. Furthermore, the selectivity for benzaldehyde achieved in the flow cell was approximately threefold higher than that of the batch reactor using the compact TiO_2 photoanode. Additionally, our investigation revealed a slightly higher benzyl alcohol conversion rate with mesoporous TiO_2 (85%) compared to compact TiO_2 (82%), attributed to the mesoporous structure's increased surface area and porosity, facilitating enhanced light absorption and reaction sites. Conversely, the denser structure of compact films helped suppress undesired side reactions on the photoanode surface, resulting in slightly higher selectivity. To sum up, these findings highlight the potential of tailored photoanodes in continuous-flow microchannels for promoting efficient and rapid PEC conversions compared to traditional PEC cells.

Data availability

The data that support the findings of this study are available from the corresponding author, P. V., upon reasonable request.

Conflicts of interest

There are no conflicts to declare.

Acknowledgements

This research was funded by the National Research Council of Thailand (NRCT) and Chulalongkorn University (Grant number N42A650267) and Thailand Science research and Innovation Fund Chulalongkorn University (No. 6641/2566).

References

1 H. Khan, S. Bera, M. Jung and S. Kwon, Rational Design of Photoanodes to Produce Value-Added Chemicals Coupled with Hydrogen, *ChemElectroChem*, 2024, **11**(13), e202400239, DOI: **10.1002/celc.202400239**.

Open Access Article. Published on 24 March 2025. Downloaded on 2/22/2026 7:25:42 PM. This article is licensed under a Creative Commons Attribution-NonCommercial 3.0 Unported Licence.

2 Z. Wu, J. Wang, Z. Zhou and G. Zhao, Highly Selective Aerobic Oxidation of Biomass Alcohol to Benzaldehyde by an *in situ* Doped Au/TiO_2 Nanotube Photonic Crystal Photoanode for Simultaneous Hydrogen Production Promotion, *J. Mater. Chem. A*, 2017, **5**(24), 12407–12415, DOI: **10.1039/C7TA03252H**.

3 A. M. M. I. Qureshy and I. Dincer, Development of a New Solar Photoelectrochemical Reactor Design for More Efficient Hydrogen Production, *Energy Convers. Manage.*, 2021, **228**, 113714, DOI: **10.1016/j.enconman.2020.113714**.

4 C. R. Lhermitte and K. Sivula, Alternative Oxidation Reactions for Solar-Driven Fuel Production, *ACS Catal.*, 2019, **9**(3), 2007–2017, DOI: **10.1021/acscatal.8b04565**.

5 Z. Zhou, Y.-N. Xie, W. Zhu, H. Zhao, N. Yang and G. Zhao, Selective Photoelectrocatalytic Tuning of Benzyl Alcohol to Benzaldehyde for Enhanced Hydrogen Production, *Appl. Catal., B*, 2021, **286**, 119868, DOI: **10.1016/j.apcatb.2020.119868**.

6 R. Zhang, M. Shao, Z. Li, F. Ning, M. Wei, D. G. Evans and X. Duan, Photoelectrochemical Catalysis toward Selective Anaerobic Oxidation of Alcohols, *Chem.–Eur. J.*, 2017, **23**(34), 8142–8147, DOI: **10.1002/chem.201701107**.

7 T. Li, J. Y. Mo, D. M. Weekes, K. E. Dettelbach, R. P. Jansonius, G. M. Sammis and C. P. Berlinguette, Photoelectrochemical Decomposition of Lignin Model Compound on a $BiVO_4$ Photoanode, *ChemSusChem*, 2020, **13**(14), 3622–3626, DOI: **10.1002/cssc.202001134**.

8 C. Jin, M. Han, Y. Wu and S. Wang, Solar-Driven Photoelectrochemical Conversion of Biomass: Recent Progress, Mechanistic Insights and Potential Scalability, *Energy Environ. Sci.*, 2024, **17**, 7459–7511, DOI: **10.1039/D4EE02332C**.

9 M. Farrag and R. Yahya, Selective Solar Photocatalytic Oxidation of Benzyl Alcohol to Benzaldehyde over Monodispersed Cu Nanoclusters/TiO_2/Activated Carbon Nanocomposite, *J. Photochem. Photobiol., A*, 2020, **396**, 112527, DOI: **10.1016/j.jphotochem.2020.112527**.

10 S. Higashimoto, N. Kitao, N. Yoshida, T. Sakura, M. Azuma, H. Ohue and Y. Sakata, Selective Photocatalytic Oxidation of Benzyl Alcohol and Its Derivatives into Corresponding Aldehydes by Molecular Oxygen on Titanium Dioxide under Visible Light Irradiation, *J. Catal.*, 2009, **266**(2), 279–285, DOI: **10.1016/j.jcat.2009.06.018**.

11 R. Arcas, E. Peris, E. Mas-Marzá and F. Fabregat-Santiago, Revealing the Contribution of Singlet Oxygen in the Photoelectrochemical Oxidation of Benzyl Alcohol, *Sustainable Energy Fuels*, 2021, **5**(4), 956–962, DOI: **10.1039/D0SE01322F**.

12 W. Nam, S. Oh, H. Joo, S. Sarp, J. Cho, B.-W. Nam and J. Yoon, Preparation of Anodized TiO_2 Photoanode for Photoelectrochemical Hydrogen Production Using Natural Seawater, *Sol. Energy Mater. Sol. Cells*, 2010, **94**(10), 1809–1815, DOI: **10.1016/j.solmat.2010.05.051**.

13 A. Fujishima and K. Honda, Electrochemical Photolysis of Water at a Semiconductor Electrode, *Nature*, 1972, **238**(5358), 37–38, DOI: **10.1038/238037a0**.

14 L. Luo, Z. Wang, X. Xiang, D. Yan and J. Ye, Selective Activation of Benzyl Alcohol Coupled with Photoelectrochemical Water Oxidation *via* a Radical Relay Strategy, *ACS Catal.*, 2020, **10**(9), 4906–4913, DOI: **10.1021/acscatal.0c00660**.

15 T. Li, T. Kasahara, J. He, K. E. Dettelbach, G. M. Sammis and C. P. Berlinguette, Photoelectrochemical Oxidation of Organic Substrates in Organic Media, *Nat. Commun.*, 2017, **8**(1), 390, DOI: **10.1038/s41467-017-00420-y**.

16 H. Li, C. Lin, Y. Yang, C. Dong, Y. Min, X. Shi, L. Wang, S. Lu and K. Zhang, Boosting Reactive Oxygen Species Generation Using Inter-Facet Edge Rich WO_3 Arrays for Photoelectrochemical Conversion, *Angew. Chem., Int. Ed.*, 2023, **62**(1), e202210804, DOI: **10.1002/anie.202210804**.

17 I. Merino-Garcia, S. Castro, A. Irabien, I. Hernández, V. Rodríguez, R. Camarillo, J. Rincón and J. Albo, Efficient Photoelectrochemical Conversion of CO_2 to Ethylene and Methanol Using a Cu Cathode and TiO_2 Nanoparticles Synthesized in Supercritical Medium as Photoanode, *J. Environ. Chem. Eng.*, 2022, **10**(3), 107441, DOI: **10.1016/j.jece.2022.107441**.

18 H. Tateno, Y. Miseki and K. Sayama, Photoelectrochemical Oxidation of Benzylic Alcohol Derivatives on $BiVO_4$/WO_3 under Visible Light Irradiation, *ChemElectroChem*, 2017, **4**(12), 3283–3287, DOI: **10.1002/celc.201700710**.

19 F. Njoka, S. Ookawara and M. Ahmed, Influence of Design and Operating Conditions on the Performance of Tandem Photoelectrochemical Reactors, *Int. J. Hydrogen Energy*, 2018, **43**(3), 1285–1302, DOI: **10.1016/j.ijhydene.2017.11.168**.

20 S. Haussener, C. Xiang, J. M. Spurgeon, S. Ardo, N. S. Lewis and A. Z. Weber, Modeling, Simulation, and Design Criteria for Photoelectrochemical Water-Splitting Systems, *Energy Environ. Sci.*, 2012, **5**(12), 9922, DOI: **10.1039/c2ee23187e**.

21 N. Ibrahim, S. K. Kamarudin and L. J. Minggu, Biofuel from Biomass *via* Photo-Electrochemical Reactions: An Overview, *J. Power Sources*, 2014, **259**, 33–42, DOI: **10.1016/j.jpowsour.2014.02.017**.

22 F. Li, Y. Wang, J. Du, Y. Zhu, C. Xu and L. Sun, Simultaneous Oxidation of Alcohols and Hydrogen Evolution in a Hybrid System under Visible Light Irradiation, *Appl. Catal., B*, 2018, **225**, 258–263, DOI: **10.1016/j.apcatb.2017.11.072**.

23 L. Xiao, Q. Zhang, P. Chen, L. Chen, F. Ding, J. Tang, Y.-J. Li, C.-T. Au and S.-F. Yin, Copper-Mediated Metal-Organic Framework as Efficient Photocatalyst for the Partial Oxidation of Aromatic Alcohols under Visible-Light Irradiation: Synergism of Plasmonic Effect and Schottky Junction, *Appl. Catal., B*, 2019, **248**, 380–387, DOI: **10.1016/j.apcatb.2019.02.012**.

24 R. Zhang, Y. Liu, Z. Wang, P. Wang, Z. Zheng, X. Qin, X. Zhang, Y. Dai, M.-H. Whangbo and B. Huang, Selective Photocatalytic Conversion of Alcohol to Aldehydes by Singlet Oxygen over Bi-Based Metal-Organic Frameworks under UV-vis Light Irradiation, *Appl. Catal., B*, 2019, **254**, 463–470, DOI: **10.1016/j.apcatb.2019.05.024**.

25 J. Zou, Z. Wang, W. Guo, B. Guo, Y. Yu and L. Wu, Photocatalytic Selective Oxidation of Benzyl Alcohol over

© 2025 The Author(s). Published by the Royal Society of Chemistry

Open Access Article. Published on 24 March 2025. Downloaded on 2/22/2026 7:25:42 PM.
This article is licensed under a Creative Commons Attribution-NonCommercial 3.0 Unported Licence.

ZnTi-LDH: The Effect of Surface OH Groups, *Appl. Catal., B*, 2020, **260**, 118185, DOI: 10.1016/j.apcatb.2019.118185.

26 F. Zhang, J. Li, H. Wang, Y. Li, Y. Liu, Q. Qian, X. Jin, X. Wang, J. Zhang and G. Zhang, Realizing Synergistic Effect of Electronic Modulation and Nanostructure Engineering over Graphitic Carbon Nitride for Highly Efficient Visible-Light H_2 Production Coupled with Benzyl Alcohol Oxidation, *Appl. Catal., B*, 2020, **269**, 118772, DOI: 10.1016/j.apcatb.2020.118772.

27 Q. Lin, Y.-H. Li, M.-Y. Qi, J.-Y. Li, Z.-R. Tang, M. Anpo, Y. M. A. Yamada and Y.-J. Xu, Photoredox Dual Reaction for Selective Alcohol Oxidation and Hydrogen Evolution over Nickel Surface-Modified $ZnIn_2S_4$, *Appl. Catal., B*, 2020, **271**, 118946, DOI: 10.1016/j.apcatb.2020.118946.

28 L. Zhang, D. Jiang, R. M. Irfan, S. Tang, X. Chen and P. Du, Highly Efficient and Selective Photocatalytic Dehydrogenation of Benzyl Alcohol for Simultaneous Hydrogen and Benzaldehyde Production over Ni-Decorated $Zn_{0.5}Cd_{0.5}S$ Solid Solution, *J. Energy Chem.*, 2019, **30**, 71–77, DOI: 10.1016/j.jechem.2018.03.014.

29 H. Hao, L. Zhang, W. Wang, S. Qiao and X. Liu, Photocatalytic Hydrogen Evolution Coupled with Efficient Selective Benzaldehyde Production from Benzyl Alcohol Aqueous Solution over ZnS–Ni_xS_y Composites, *ACS Sustainable Chem. Eng.*, 2019, 7(12), 10501–10508, DOI: 10.1021/acssuschemeng.9b01017.

30 M. I. Jaramillo-Gutiérrez, E. P. Rivero, M. R. Cruz-Díaz, M. E. Niño-Gómez and J. A. Pedraza-Avella, Photoelectrocatalytic Hydrogen Production from Oilfield-Produced Wastewater in a Filter-Press Reactor Using TiO_2-Based Photoanodes, *Catal. Today*, 2016, **266**, 17–26, DOI: 10.1016/j.cattod.2015.12.008.

31 W. Zhang, Y. Lin, R. Chen, X. Zhu, D. Ye, Y. Yang, J. Li, Y. Yu and Q. Liao, Self-Doped TiO_2 Nanotube Array Photoanode for Microfluidic All-Vanadium Photoelectrochemical Flow Battery, *J. Electroanal. Chem.*, 2021, **897**, 115598, DOI: 10.1016/j.jelechem.2021.115598.

32 J. Li, Y. Lin, R. Chen, X. Zhu, D. Ye, Y. Yang, Y. Yu, D. Wang and Q. Liao, Solar Energy Storage by a Microfluidic All-Vanadium Photoelectrochemical Flow Cell with Self-Doped TiO_2 Photoanode, *J. Energy Storage*, 2021, **43**, 103228, DOI: 10.1016/j.est.2021.103228.

33 Y.-W. Su, B. K. Paul and C. Chang, Investigation of CdS Nanoparticles Formation and Deposition by the Continuous Flow Microreactor, *Appl. Surf. Sci.*, 2019, **472**, 158–164, DOI: 10.1016/j.apsusc.2018.02.157.

34 T. Hanamorn and P. Vas-Umnuay, CFD Modeling and Simulation of Benzyl Alcohol Oxidation Coupled with Hydrogen Production in a Continuous-Flow Photoelectrochemical Reactor, *Sci. Rep.*, 2023, **13**(1), 22568, DOI: 10.1038/s41598-023-50102-7.

35 N. Khothong, T. Anantamongkolchai and P. Vas-Umnuay, Morphology and Structure Controlled Fabrication of Cu_2ZnSnS_4 Thin Films by Convective Assembly Deposition, *Ceram. Int.*, 2019, **45**(5), 6102–6110, DOI: 10.1016/j.ceramint.2018.12.084.